Interacting-boson-fermion-fermion model description of $^{140}La_{83}$ and comparison with levels populated by beta decay and neutron capture

R. A. Meyer*
Division of High Energy and Nuclear Physics, U.S. Department of Energy, Washington, D.C. 20545 and Nuclear Chemistry Division, Lawrence Livermore National Laboratory, Livermore, California 94550

K. V. Marsh
Nuclear Chemistry Division, Lawrence Livermore National Laboratory, Livermore, California 94550

H. Seyfarth and S. Brant†
Institut für Kernphysik, Kernforschungsanlage Jülich, 5170 Jülich, Federal Republic of Germany

M. Bogdanović
The Boris Kidrič Institute of Nuclear Sciences, 11001 Belgrade, Yugoslavia

V. Paar
Prirodoslovno-matematički fakultet, University of Zagreb, 41000 Zagreb, Yugoslavia and Lawrence Livermore National Laboratory, Livermore, California 94550
(Received 27 September 1989)

We have studied the levels of ^{140}La populated in the beta decay of ^{140}Ba by gamma-ray spectroscopy, which included Compton-suppression gamma-ray spectra of ^{140}Ba sources that were continuously eluted of the ^{140}La daughter activity using ion-exchange chromatographic techniques. The study of the gamma-ray deexcitation of the low-energy levels was completed by a measurement of the low-energy gamma-ray spectrum following thermal neutron capture on ^{139}La. Also, we have performed calculations using the interacting-boson-fermion-fermion model. When we compare the model predictions with the levels and their properties, which we have determined, we find better agreement than has been obtained using quasiparticle-vibrational models.

I. INTRODUCTION

There have been a large number of theoretical investigations concerning odd-odd nuclei but few based on the interacting-boson model.[1–26] Further, except for odd-odd nuclei that abut doubly closed shells, nuclei such as ^{140}La have been difficult to describe in detail. As shown in Fig. 1, where the levels of ^{140}La are juxtaposed with the levels of its $N=83$ isotones,[27–33] the low-energy levels of ^{140}La reflect the fact that it is the midsubshell nucleus, which lies between $_{50}$Sn and the subshell closure at $_{64}$Gd. As such, ^{140}La should serve as a good test for symmetry models such as the interacting-boson-fermion-fermion model (IBFFM). We have therefore performed IBFFM calculations for ^{140}La.

In order to test our IBFFM calculations, detailed information on the deexcitation of the low-energy levels is critical. Unfortunately, such detailed information has not been available. For example, of the experimental studies of the levels of ^{140}La, which have been summarized in the recent Nuclear Data Sheets (NDS) by Peker,[27] all but one of the recent spectroscopy investigations of the ^{140}Ba-^{140}La system have been concerned with determination of the absolute intensities of the more abundant gamma rays for metrological uses.[34–37] Only Adam and co-workers[38] have made a detailed investigation of the gamma rays below around 100 keV. A number of low-energy ($E_x < 600$ keV) transitions, which are critical to testing the present IBFFM calculations, have not been observed and limits have only been set on the intensities of some.

The lack of observation of low-energy low-intensity transitions is mainly due to two factors. First, the parent-daughter ^{140}Ba-^{140}La activity occurs in transient equilibrium and the daughter ^{140}La decay to ^{140}Ce produces a large number of high-energy gamma rays. The second factor is that, even if the ^{140}La daughter activity is suppressed, the most intense gamma ray resulting from the beta decay of ^{140}Ba to levels of ^{140}La is the highest-energy gamma ray and hence it produces a high Compton continuum in the low-energy portion of the spectra. In order to overcome these factors, we have devised a special technique to continuously suppress the presence of the ^{140}La daughter activity and simultaneously measure the gamma rays using a Compton-suppression spectrometer. Here we present the results of our gamma-ray spectroscopy studies of the low-energy levels of ^{140}La populated in the beta decay of ^{140}Ba.

The earlier study[12] of the gamma rays emitted after thermal neutron capture in ^{139}La has been extended by measurements of the gamma-ray and conversion-electron spectra with use of the spectrometers at the High Flux

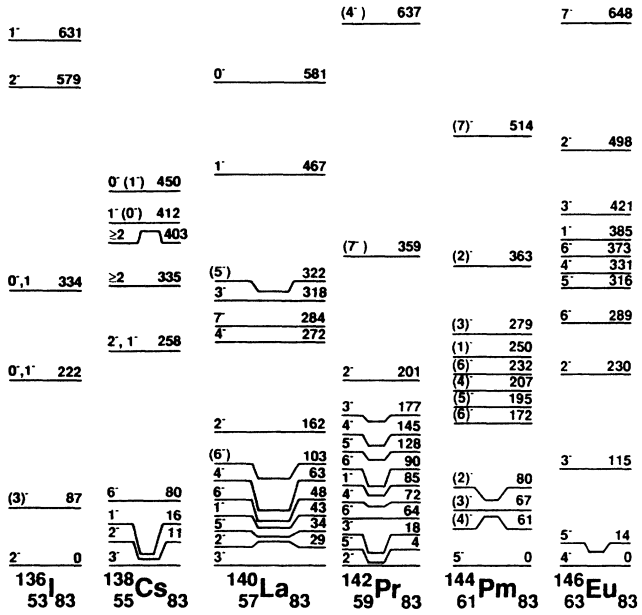

FIG. 1. Experimentally known levels of the $N=83$ isotones below 700 keV (data taken from Refs. 27–40 and this work).

Reactor of the Institut Laue Langevin (ILL) in Grenoble, France. The results, covering the energy ranges $30 < E_\gamma < 120$ keV and $20 < E_{CE} < 1000$ keV are presented elsewhere[39] while a preliminary level scheme has been presented.[40] The decrease in the gamma-ray detection efficiency with decreasing gamma-ray energy (< 100 keV) and the increasing uncertainty in the gamma-ray intensity determination, caused by self-absorption in the target, required us to perform a separate, additional, measurement of the low-energy gamma-ray spectrum. The main aim of the present study, performed at an external beam of the FRJ-2 research reactor of Kernforschungsanlage Julich (KFA), was to detect hitherto unobserved low-energy transitions from the decay of the low-energy levels in ^{140}La and in particular the 63-keV 4^- and 49-keV 6^- levels. Both the latter two levels are populated from the 3^+, 4^+ thermal neutron-capture state, whereas only the first level is populated, albeit very weakly, following the beta decay of ^{140}Ba. The results of this study, which also yields lower uncertainties for the gamma-ray intensities of the intense low-energy transitions, are presented herein.

II. EXPERIMENTS

A. Beta decay of ^{140}Ba

The sources of ^{140}Ba were produced by two separate methods. In the first, Ba was isolated from the fission products produced in an underground nuclear explosion using standard radiochemical procedures.[41] These sources were sealed in counting planchets. Gamma-ray spectra were measured with a large-volume Ge(Li) spectrometer, a Compton-suppression spectrometer,[42] and a high-resolution, low-energy, photon spectrometer. Multigamma-ray standards[43,44] were measured simultaneously with the ^{140}La sources in order to obtain precise energy values. The gamma-ray energies and relative intensities were determined from the spectra taken on all systems. The photopeak efficiencies for the Ge(Li) detectors and the nonlinearity corrections for the analyzer systems were measured independently using standard calibration sources.[44] Spectra were analyzed with the code GAMANAL.[45]

A second set of sources was prepared in which the ^{140}La was continuously removed from the ^{140}Ba parent by ion-exchange separation. The experimental setup is shown schematically in Fig. 2. The ion-exchange column was located directly under the entrance aperture to the Compton-suppression spectrometer. The up-stream end of the ion-exchange column was connected to a pressurized source of eluant and the down-stream end was connected to a waste bottle housed in a Pb shield. Preliminary experiments established that a sufficiently rapid and complete separation could be obtained using a short column of Dowex 50×10 cation exchange resin and using an eluant consisting of a pH 5 solution of 0.5 mol alpha-hydroxy isobuteric acid in 50% ethyl alcohol (alcoholic alpha-But). All of the apparatus near the source was made of plastic to minimize scattering and absorption of the low-energy gamma rays from the ^{140}Ba. The column itself was made from a 3-cm^3 plastic syringe barrel with a small glass wool plug at the end. This plug supported approximately 2.5 cm of Dowex 50×10 100-200 mesh resin with a layer of colloidal resin (settling rate 3–8 mm/min) about 0.7 cm thick on top.

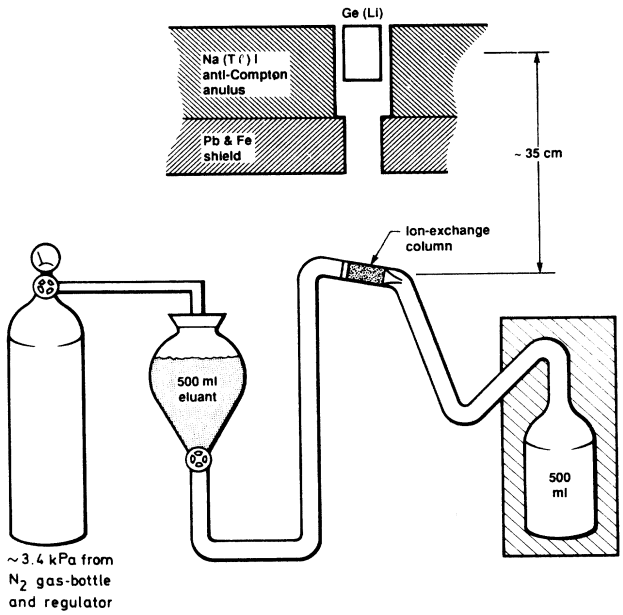

FIG. 2. Diagrammatic sketch of the experimental setup for measuring the Compton-suppression spectra of a ^{140}Ba-^{140}La source in which the daughter ^{140}La activity was continuously eluted from the ^{140}Ba parent activity. The ^{140}Ba activity, contained on the ion-exchange resin, was eluted with a solution of alcoholic alpha-But under a pressure of $\sim\frac{1}{2}$ psi. The column was aligned with the central axis of the Compton-suppression spectrometer's aperture (see text).

For the Compton-suppression spectroscopy measurements, first a source of approximately 2 mCi of ^{140}Ba-^{140}La in alcoholic alpha-But solution was equilibrated in a centrifuge tube with about 0.2 ml of colloidal resin and centrifuged. Then the solution, containing virtually all of the ^{140}La, was discarded and the resin containing the ^{140}Ba was transferred as a slurry to the top of the column with a transfer pipette. This gave a total thickness of about 1 cm of colloidal resin at the top of the column, sufficient for good separation of the Ba and La, but thin enough to permit adequate flow at low pressure. Finally, once all the connections were made, any air bubbles worked out, and the column was flowing properly, accumulation of the spectrum was begun. From time to time over the course of a measurement the accumulated spectrum was checked for evidence of the 487- or 1596-keV gamma rays of ^{140}La. If they appeared to be becoming too intense, pressure was increased slightly to increase flow rate of the eluant. The flow rate could be monitored quite closely by counting drops of eluant from the end of the column that occurred over a specific period of time. A typical experiment ran continuously for four days at a flow rate of 5 ml/h.

B. Neutron-capture gamma-ray experiments

The low-energy gamma-ray spectra from the thermal neutron capture in ^{139}La have been measured at the external neutron beam facility[46] at the FRJ-2 research reactor of KFA Julich. A thin target was produced by pressing a homogeneous mixture of 10 mg of La_2O_3 and 10 mg of deuterized polyethylene into a tablet of 17.7 mg/cm^2 (7.3 mg/cm^2 of La). The natural abundances and thermal neutron-capture cross sections[47] of ^{138}La [0.09% and 57.2(57) b, respectively] and ^{139}La [99.91% and 8.93(4) b, respectively] yield 0.57% and 99.43% capture contribution in ^{138}La and ^{139}La, respectively, and thus allow the use of natural target material. The target was suspended at an angle of 30° to the axis of the vertical neutron beam within the neutron shielding tube in front of a 1.4-cm^3 HP-Ge detector. Details of the setup and the relative detection efficiency have been given elsewhere.[48]

III. EXPERIMENTAL RESULTS AND LEVEL SCHEME

In Fig. 3 we show a typical spectrum of the eluted ^{140}Ba source taken with the Compton-suppression spectrometer. In Table I we give the gamma-ray energies and intensities that we measure for the decay of ^{140}Ba to the levels of ^{140}La, and in Fig. 4 we show the placement of the gamma rays in the ^{140}La level scheme.

In general, our values for the intensities of the more intense gamma rays agree with those reported by Debertin and co-workers.[34] Our increased sensitivity is illustrated by the fact that we can measure an intensity of the 418-keV gamma ray as being 0.15 units relative to the 537-keV gamma ray having 1000 units, while Adam *et al.*[38] only report a limit of ≤ 0.4 units. Also, we note that the precision gamma-ray energies, which we measure using techniques described elsewhere,[43,44] have been adjusted to the remeasurement of the 411-keV fiducial of ^{196}Au reported by Kessler *et al.*[49]

The low-energy part of the gamma-ray spectrum resulting from thermal neutron capture in the setup described in Sec. II B is shown in Fig. 5. The energy calibration has been achieved with known gamma rays[43,44,54] from ^{57}Co, ^{152}Eu, and ^{241}Am registered in a separate run simultaneously with those from the La(n_{th}, gamma) reaction. A third-order correction was applied to take into account the nonlinearity of the electronic system. From the relative gamma-ray intensities, corrected for self-absorption in the target, the absolute intensities were obtained by normalizing to the strong gamma rays of the 328.8- and 487.0-keV ^{140}Ce gamma rays, which are emitted[27] with an intensity of 20.6(4) and 44.3(8) per 100 de-

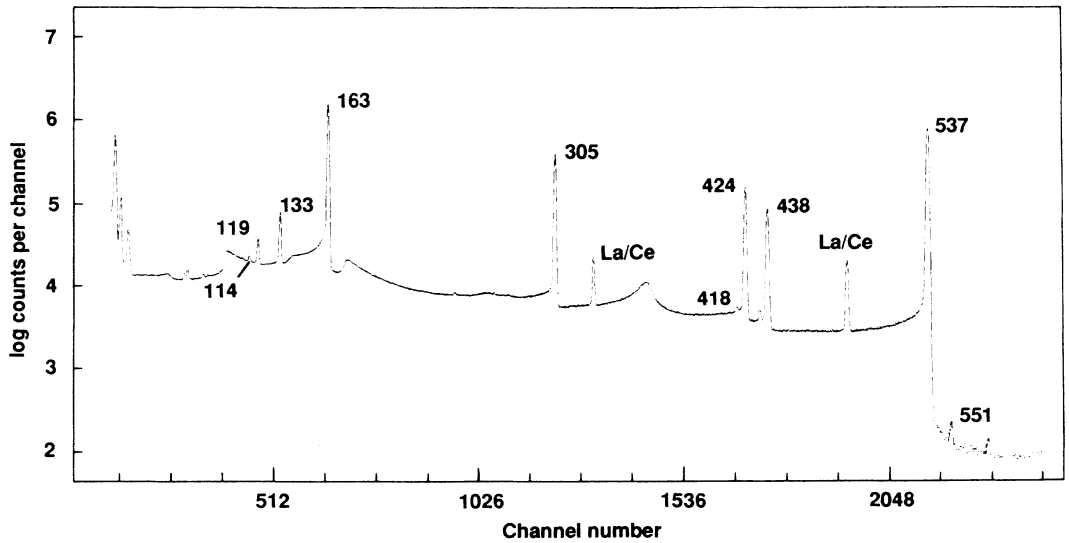

FIG. 3. Compton-suppression spectrum of a ^{140}Ba-^{140}La source enriched in ^{140}Ba by ion-exchange techniques. The photopeaks labeled La/Ce belong the decay of ^{140}La to ^{140}Ce (see text).

cays, respectively, and a $t_{1/2}=1.6781(3)$ d. The resulting gamma-ray and x-ray energies and intensities are presented in Table II.

The 14.18(8)-keV gamma ray is observed for the first time. It corresponds to the 100% deexcitation from the 48.9-keV 6^- level to the 34.7-keV 5^- levels [$\Delta E=14.209(6)$ keV level energy difference[27]]. The assumption of a pure $M1$ character for this transition yields the total transition intensity as $20\pm4/100$ neutrons, in agreement with the total population of the 48.9-keV level.[39] The spectral shape, shown in the Fig. 5 inset, shows that in the ^{139}La(n_{th}, gamma) reaction, the 13.8-keV transition (between the 43.8-keV 1^- and 30.3-keV 2^- levels)

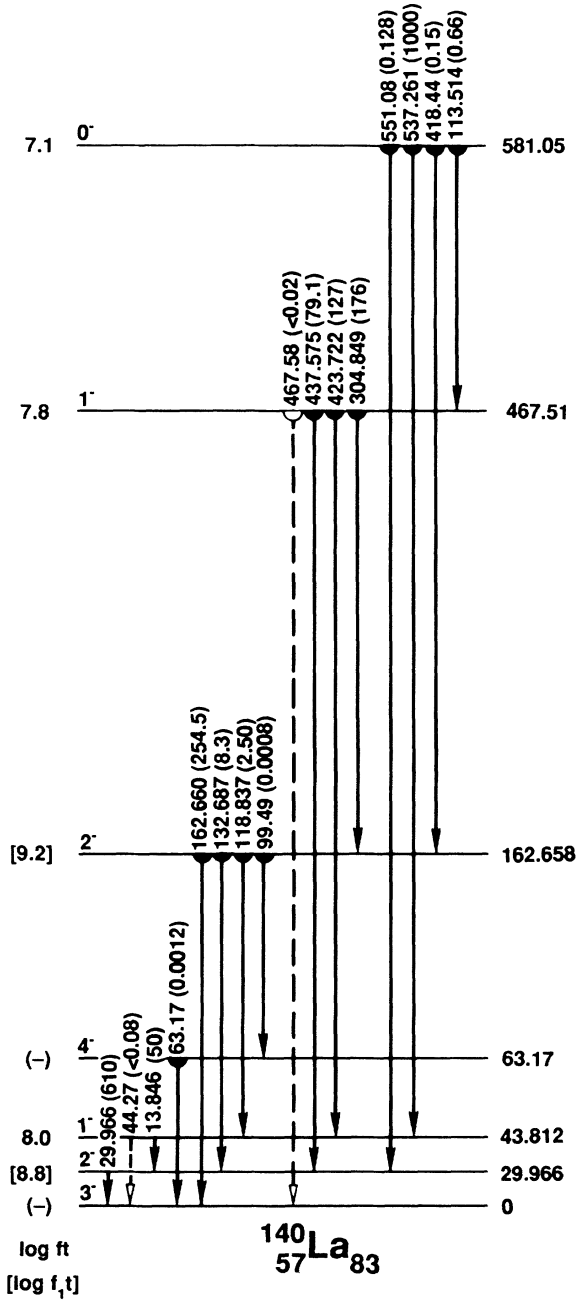

FIG. 4. Levels of ^{140}La populated by the beta decay of ^{140}Ba.

TABLE I. Gamma-ray energies and intensities observed from the beta decay of ^{140}Ba to levels of ^{140}La.

Energy[a] (keV)	Intensity[b] (relative)	Assignment From	Assignment To
13.846(15)[c]	50(7)[d]	44	30
29.966(1)[c]	610(40)[d]	30	GS
44.27(−)[e]	<0.08	44	GS
63.17(22)	0.0012(6)	63	GS
99.49(2)	0.0008(5)	163	63
113.514(31)	0.66(5)	581	467
118.837(3)	2.50(3)	162	44
132.687(1)	8.3(2)	162	30
162.660(1)	254.5(29)	162	GS
183.83(9)[f]	0.04(2)[f]		
275.18(18)[f]	0.015(6)[f]		
304.849(3)	176(2)	467	162
418.44(4)	0.15(1)	581	162
423.722(1)	127(1)	67	44
437.575(2)	79.1(4)	467	30
467.58(−)[e]	<0.02	467	GS
537.261(9)	1000(3)	581	44
551.08(4)	0.128(8)	581	30
699.89(13)[f]	0.034(9)[f]		

[a]The gamma-ray energies have been corrected for the new value of the ^{197}Au 411-keV gamma-ray energy measured by Kessler *et al.* (Ref. 49).

[b]Intensities are relative to the 537-keV gamma ray. For absolute intensities, multiply by 0.024 39(22) [see Debertin *et al.* (Ref. 34)].

[c]Energy measured by Kern and Mauron (Ref. 50).

[d]This intensity is consistent with the recent measurements of Adam *et al.* (Ref. 38).

[e]This gamma ray was not observed in our measurements. The energy represents the level energy difference of the levels given in the assignment column.

[f]These gamma rays were observed in the chemically enriched Ba sources that were measured with the Compton-suppression spectrometer. Their association with the ^{140}Ba decay must be taken as purely tenuous until the gamma rays are observed to belong in the ^{140}La system.

is appreciably weaker than the 14.2-keV transition. This is in contrast to that observed in the beta decay of ^{140}Ba, where the 48.9-keV 6^- state is not populated at all. Thermal neutron capture in ^{139}La with a $\frac{7}{2}^+$ g.s. leads, by 99%, to the formation of the 4^+ capture state.[47] The lower spin difference of the 48.9-keV 6^- level ($\Delta J=2$) favors the population of this state as compared to the 43.8-keV 1^- level ($\Delta J=3$), which explains the observed intensities.

The calculated x-ray intensities were used to deduce the intensities of the 34.7- and 38.7-keV gamma rays from the unresolved gamma-ray–x-ray doublets. The observed La $K\alpha_2/K\alpha_1$ intensity ratio of 0.536(5) is in good agreement with the calculated value of 0.544 (estimated error less than 2%).[55] This result and the fitted $K\alpha_2$ and $K\alpha_1$ energies of Table II demonstrate the quality of the data deduced from the multiplets at 34 and 38 keV. The calculated Ce $K\alpha_2/K\alpha_1$ intensity ratio of 0.546(11) and the observed intensities given in Table II yield a gamma-ray intensity of 0.23(11)/100 neutrons for the 34.6-keV

transition. The fitted average energy, the total intensity, and the energies of the two components, which contribute to the unresolved peak, yield a gamma-ray intensity of 0.39(12)/100 neutrons [(54±16)% of the peak intensity]. Both values are in agreement and yield finally a gamma-ray intensity of 0.31(8)/100 neutrons for the 34.6-keV transition. The calculated ratios[56] La $K\beta_2/(K\beta_3+K\beta_1)=0.213$ and La $K\beta_2/(K\alpha_2+K\alpha_1)=0.039$ can be used to derive the gamma-ray intensity of the 38.7-keV transition. They yield 0.074(21) and 0.091(17)/100 neutrons, respectively, or the weighted average 0.084(13)/100 neutrons. A possible 40.6-keV photopeak from a weak transition between the 103.8-keV 6^- level and the 63.2-keV 4^- level, not observed in the earlier ^{139}La(n_{th}, gamma) study,[12] may be obscured by the Eu $K\alpha_2$ peak. Comparison of the measured Eu $K\alpha_2/K\alpha_1$ ratio (see Fig. 5) of 0.51 and the calculated ratio[55,56] of 0.55(1) yields an upper limit of 0.004/100 neutrons for the 40.6-keV $E2$ transition.

The photopeaks which are labeled "esc" in Fig. 5 can be interpreted as Ge K x-ray escape peaks. Their energies are lower by 11.0 and 9.9 keV than those of the intense peaks at 30.0, 33.0 (La $K\alpha_1$), 33.4 (La $K\alpha_2$), and 37.8 (La $K\beta_3+K\beta_1$) keV. These energy differences correspond to the Ge $K\beta$ and $K\alpha$ x-ray energies of 10.981 and 9.876 keV, respectively.[57] The observed ratios of the sum of the peak areas with energy differences of −11.0 and −9.9 keV to the peak area of the true photopeaks are (photopeak energy in brackets [ ]) 0.045(7) [30.0], 0.036(2) [33.0], 0.025(2) [33.4], and 0.014(2) [37.8]. These ratios agree with the experimental and calculated ratios given in Ref. 58 for the escape peak to photopeak ratios, which confirms this interpretation. Therefore the transition of 26.60 between the 602.0- and 575-keV levels, given in the preliminary level scheme,[40] must be omitted because the observed intensity corresponds to what is expected for the Ge $K\beta$ escape peak of the 37.8-keV photopeak.

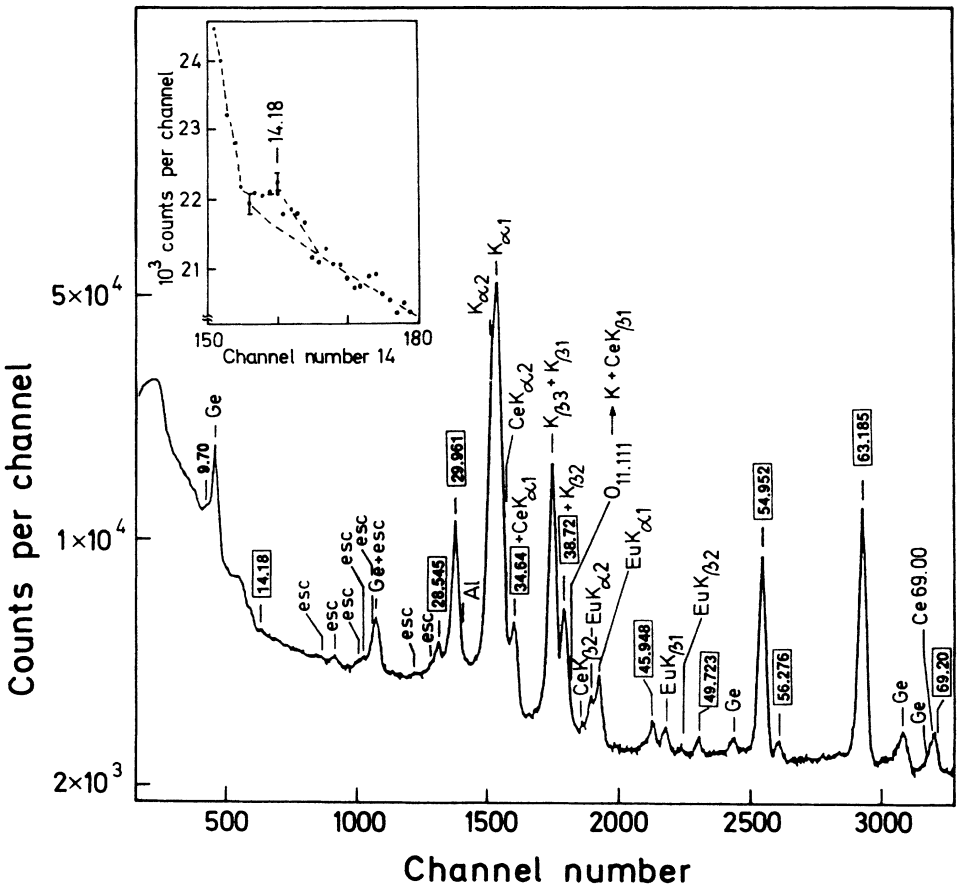

FIG. 5. The low-energy spectrum from thermal neutron capture in the experimental setup described in Sec. II. The energies of the photopeaks from the La(n, gamma) reaction are given in boxes. The photopeaks labeled Ge and Al result from neutron capture in the HP-Ge detector (Ref. 51) and the Al cryostat material (Ref. 52). The photopeaks labeled with Eu x-ray components result from a tiny Eu impurity in the target [the most intense ^{151}Eu(n, gamma) photopeaks of 89.849 and 77.258 keV (Ref. 53) are observed in the higher section of the spectrum, too, and yield an Eu impurity on the order of 10 ppm]. Photopeaks labeled by an x-ray component only are from La, whereas those with the additional label Ce are emitted after the beta decay of La. The labels "esc" denote photopeaks which correspond to the intense low-energy photopeaks with an escape of a Ge K quantum from the detector (E_{gamma} less 9.876 and E_{gamma} less 10.981 keV, respectively). The inset shows the 14.18(8) keV line with four channels summed.

TABLE II. Low-energy gamma rays and K x rays emitted after thermal neutron capture in natural La and observed with a 1.4-cm^3 HP-Ge detector.

Assignment[a]	Energy in keV This work	Note b	Intensity per 100n This work	Note c	Placement From	To
^{140}La		13.846(15)[d]	<0.09		43.8	30.0
^{140}La	14.18(8)		0.39(8)		48.9	34.7
^{140}La	28.545(22)	28.536(7)	0.145(15)	0.16(6)	63.2	34.7
^{140}La	29.961(5)	29.9640(7)	2.39(7)	2.1(8)	30.0	0.0
La$K\alpha_2$	33.021(9)	33.0340[e]	8.09(7)			
La$K\alpha_1$	33.443(6)	33.4419[e]	15.08(13)			
Ce$K\alpha_2$	34.20(5)	34.2788[e]	0.27(6)			
^{140}La		34.6467(13)		0.27(8)	34.7	0.0
	34.680(12)		0.73(2)[f]			
Ce$K\alpha_1$		34.7196[e]				
La$K\beta_3$						
	37.786(6)	37.7736[e]	4.33(7)			
La$K\beta_1$						
^{140}La		38.6948(15)			711.6	673.0
	38.729(8)		0.995(16)[f]			
La$K\beta_2$		38.7283[e]				
^{140}La		40.63[g]	<0.004		103.8	63.2
^{140}La		43.82[g]	<0.003		43.8	0.0
^{140}La	45.948(18)	45.9(1)[c]	0.169(7)	0.17(6)	318.2	272.3
^{140}La	49.723(23)		0.070(8)		322.0	272.3
^{140}La	54.952(6)	54.9443(11)	2.02(7)	2.1(6)	103.8	48.9
^{140}La	56.276(33)	56.246(7)	0.065(6)	0.16(4)	658.2	602.0
^{140}La	63.185(6)	63.1791(8)	3.15(12)	3.7(7)	63.2	0.0
^{140}La	69.14(3)	69.1834(27)	0.185(15)	0.22(7)	103.8	34.7

[a]The K x-ray line designation follows that of Refs. 55 and 56.
[b]Measured with the crystal spectrometers at ILL (Refs. 39 and 40) unless labeled by another reference.
[c]From Ref. 12. The values given there are based on the cross section of 8.2(8) b for the thermal neutron capture of ^{139}La. The gamma-ray intensities given here have been reduced according to the actual value of 8.93(4) b given in Ref. 47.
[d]From Ref. 50.
[e]Calculated from the electron binding energies given in Ref. 57.
[f]The gamma-ray intensity is deduced from the total intensity (see text).
[g]The upper gamma-ray intensity limits are given for the low-intensity ($E2$) transitions.

IV. THEORETICAL DESCRIPTION OF THE LEVELS OF ^{140}La

A. Previous theoretical investigations

In the zeroth-order approximation, the four lowest multiplets in ^{140}La arise from the coupling of a neutron (n) in $f_{7/2}$ or $p_{3/2}$ orbitals to a quasiproton (p) in $g_{7/2}$ and $d_{5/2}$ orbitals. Thus the lowest-lying negative-parity states are based on the multiplets

$$(pg_{7/2}nf_{7/2})\ 0,\ldots,7\ ,$$
$$(pd_{5/2}nf_{7/2})\ 1,\ldots,6\ ,$$
$$(pg_{7/2}np_{3/2})\ 2,\ldots,5\ ,$$
$$(pd_{5/2}np_{3/2})\ 1,\ldots,4\ .$$

These proton-neutron multiplets will be referred to as gf, df, gp, and dp multiplets, respectively.

From the positive sign of the ground-state quadrupole moment of ^{139}La, $Q(\frac{7}{2}^+)=+0.22\ e$ b, it follows that the $g_{7/2}$ quasiparticle is holelike, that is $u(g_{7/2})<v(g_{7/2})$ and hence, that the $d_{5/2}$ quasiparticle is particlelike, that is $u(d_{5/2})>v(d_{5/2})$. Therefore the gf and df proton-neutron multiplets are of hole-particle and particle-particle type, respectively. If the Brennan-Bernstein rule[1] is applied, the lowest-energy level is predicted to be 6^-. Thus the experimentally observed 3^- ground state strongly violates the Brennan-Bernstein rule, revealing the complexity of the structure of ^{140}La.

In Refs. 2 and 3 the states arising from gf and df multiplets have been described by applying the parabolic rule.[4] In this description the exchange of quadrupole boson and spin-vibration boson was included in the leading order. In Ref. 2 the $0^-(1)$ and $7^-(1)$ levels were assigned to the gf parabola and the remaining levels were assigned to achieve the best fit. The resulting occupation probabilities (v^2) extracted from the parabolic rule were 0.63 and 0.42 for the $g_{7/2}$ and $d_{5/2}$ proton quasiparticles, respectively. These values are in modest agreement with the spectroscopic factors extracted from (^{3}He,d) studies,[5] which gave 0.42 and 0.21, respectively. However, this procedure predicts the ground state to be 5^-, while the experimental 2^- and 3^- levels are appreciably displaced from the predicted parabolas.[2]

Here we investigate an alternate fit to the parabolic rule, where the $3^-(1)$ ground state and the $1^-(1)$, $2^-(1)$, $4^-(1)$, $5^-(1)$, $6^-(1)$, and $7^-(1)$ levels have been fit to the gf parabola, leaving the $0^-(1)$ state out of the fitting procedure. In this case we take the quasiparticle energies of lowest states in ^{139}La and ^{139}Ba, the occupation strengths from the Reehal-Soresen parametrization[6] [$v^2(pg_{7/2})=0.612$, $v^2(pd_{5/2})=0.254$, $v^2(nf_{7/2})=0.088$, and $v^2(np_{3/2})=0.021$], and the interaction strengths as $\alpha^0(1)=0.25$ and $\alpha^0(2)=2.5$. The two lowest-energy proton-neutron parabolas that result from this procedure are presented in Fig. 6(A). In Fig. 6(B), this theoretical spectrum is compared to the low-energy experimental levels of ^{140}La.

Several investigations of the level structure of ^{140}La have been made using an odd-odd quasiparticle model (OOQM). Several attempts to extend the quasiparticle approach to odd-odd nuclei[7–9] have been made, and Struble[10] has given a detailed accounting of ^{140}La within this framework. In the latter, a residual interaction, the finite range central interaction with Gaussian shape, was used. The calculated ground state was predicted to be 6^-, which is in accordance with the Brennan-Bernstein rule. Struble concludes that the OOQM calculation underestimates configuration mixing between the $g_{7/2}$ and $d_{5/2}$ quasiproton states for spins 1, 2, and 3, and is related to the problem of relative ordering of the states.

In another recent investigation[11] the energy spectrum of ^{140}La was calculated using a weak-coupling shell model in a proton-neutron formalism with a modified surface delta interaction. As in the other previous calculations, this calculation also failed to reproduce the correct ground state. However, this calculation gave a better overall agreement with experiment for energies of the 13 lowest levels. Unfortunately, the position of higher-energy states and in particular that of the $0^-(1)$ state was not reported.[11]

A rather simplistic approach to the low-lying negative-parity states of ^{140}La directly related to experiment has been used by Jurney *et al.*[12] There, only the gf and df two-quasiparticle states were considered, and their mixing amplitudes for each state were fitted separately to the experimental (d,p) amplitudes. A second fit was made for the transitions, which are largely of $M1$ type. In this way a rather good fit to the electromagnetic and transfer data was obtained. However, there is a basic open question as to the energies corresponding to these wave functions and about the interaction that would simultaneously give these wave functions.

B. Calculation of levels within the IBFFM

Over the last decade the IBM and the IBFM have been extensively applied to the description of even-even and odd-mass nuclei.[13,14] This approach has been recently extended to odd-odd nuclei.[15–22] This new model was referred to as the IBFFM.[15–22] In a related development, a few dynamical symmetries and supersymmetries have been introduced.[17,18,21]

The IBFFM Hamiltonian reads

$$H_{\mathrm{IBFFM}}=H_{\mathrm{IBFM}}(p)+H_{\mathrm{IBFM}}(n)-H_{\mathrm{IBM}}+H_{\mathrm{res}}(pn)\ .$$

Here, $H_{\mathrm{IBFM}}(p)$ and $H_{\mathrm{IBFM}}(n)$ denote the IBFM Hamiltonians[14] for odd-mass nuclei with an odd proton and odd neutron, respectively. H_{IBM} denotes the IBM Hamiltonian,[13] and $H_{\mathrm{res}}(pn)$ denotes the residual proton-neutron interaction. In the IBFFM/OTQM computer code,[23] the following residual interactions are incorporated: multipole-multipole, surface-delta, spin-spin, spin-spin-delta, and tensor interaction.

Because we investigate the states below 1 MeV with small boson admixtures, a harmonic IBM core has been

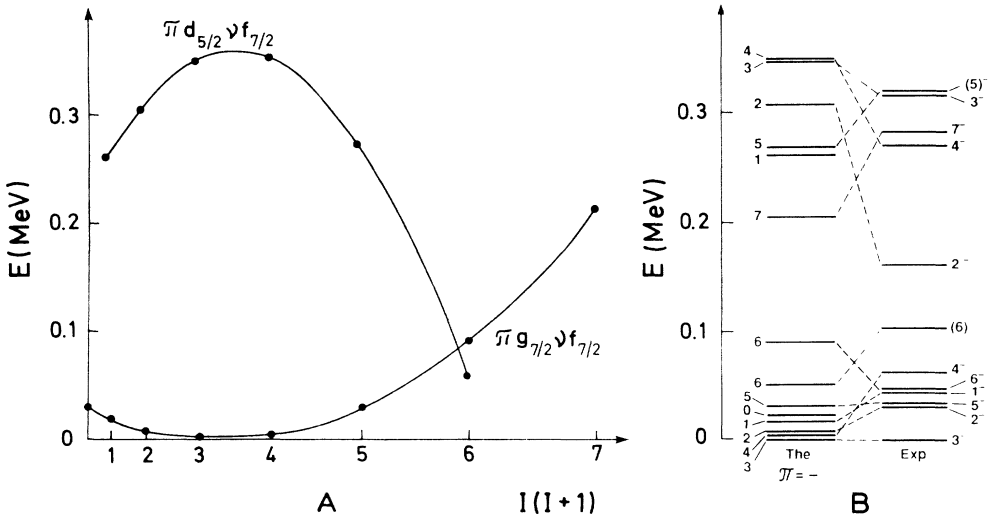

FIG. 6. (A) Application of the parabolic rule to ^{140}La with two requirements: (i) the $3^-(1)$ level is at the bottom of gf parabola and (ii) the $0^-(1)$ level is excluded from the fit. (B) Comparison of the spectrum in (A) to the experimental negative-parity levels of ^{140}La.

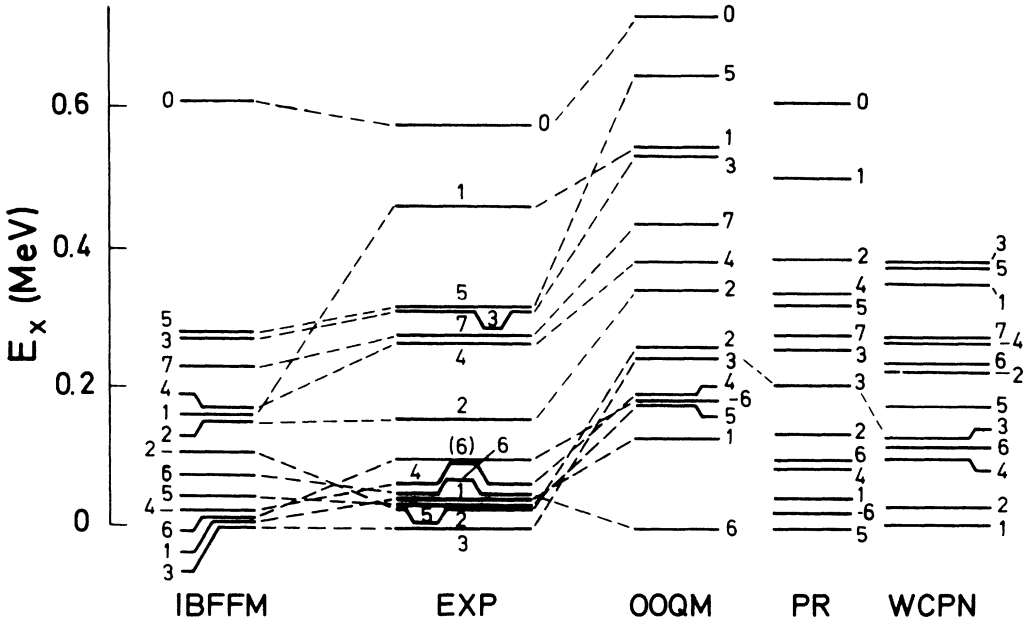

FIG. 7. IBFFM negative-parity energy spectrum of ^{140}La compared with the experimentally known energy spectrum and with the three previous calculations performed using the odd-odd quasiparticle model (OOQM) (Ref. 10), the parabolic rule (PR) (Ref. 2), and the weak-coupling shell model in the proton-neutron formalism (WCPN) (Ref. 11).

used with d-boson energy given by the energy of the first excited state in the core nucleus $^{138}Ba_{82}$. Six valence-shell particles in the core determine the boson number as $N=3$. The quasiparticle energy differences were taken as $\epsilon[p(d_{5/2}-g_{7/2})]=0.105$ MeV and $\epsilon[n(p_{3/2}-f_{7/2})]=0.95$ MeV and the occupancies were taken as $v^2(pg_{7/2})=0.8$, $v^2(pd_{5/2})=0.1$, $v^2(nf_{7/2})=0.088$, and $v^2(np_{3/2})=0.021$. The quasiparticle energies and proton occupation probabilities are close to the standard BCS parametrization,[6] but slightly adjusted to ^{140}La. The neutron occupation probabilities were chosen according to Ref. 6. The interaction strengths employed in the present calculation, determined in order to get an overall

TABLE III. Static moments of low-lying states of ^{140}La calculated in the IBFFM. The only available experimental static moments (Ref. 27) are $Q\{3(1)\}=0.103(11)$ e b (cf 0.11 predicted) $\mu\{3(1)\}=0.730(15)\mu_N$ (cf. 0.68 predicted).

Level	Q (e b)	μ (μ_N)
$3^-(1)$	0.11	0.68
$2^-(1)$	0.14	0.14
$5^-(1)$	0.05	1.08
$1^-(1)$	−0.12	−2.08
$6^-(1)$[a]	−0.08	1.36
$4^-(1)$	0.11	0.89
$6^-(2)$[a]	−0.87	2.47
$2^-(2)$	0.11	−0.16
$4^-(2)$	−0.28	1.29
$7^-(1)$	−0.05	1.51
$3^-(2)$	0.07	0.23

[a]The sequence of the calculated 6^- states has been interchanged (see text).

TABLE IV. Branching ratios for the low-energy, negative-parity levels in ^{140}La, calculated within the IBFFM, compared with the experimental data. The $J(n)$ identification of the observed levels, given in the first two columns to the left, is assigned to the IBFFM levels in accordance with Fig. 7. For each level the branching ratios are normalized to the most intense experimental transition.

Transition		Branching ratio[a]	
From	To	Expt.	IBFFM
1(1)	3(1)	<0.16	0.001
	2(1)	100	100
4(1)	3(1)	100	100
	2(1)		10^{-6}
	5(1)	4.6(5)	9
	6(1)[a]		10^{-7}
6(2)[a]	5(1)	9(1)	680
	6(1)[a]	100	100
	4(1)	<0.2	2×10^{-4}
2(2)	3(1)	100	100
	2(1)	3.3(1)	16
	1(1)	0.98(2)	79
	4(1)	0.0003(2)	0.001
1(2)	3(1)	<0.01	0.001
	2(1)	44.9(6)	72
	1(1)	72.2(10)	61
	2(2)	100	100
	3(2)		0.003
0(1)	2(1)	0.0128(6)	0.04
	1(1)	100	100
	2(2)	0.015(1)	0.006
	1(2)	0.066(5)	4.9

[a]The sequence of the calculated 6^- states have been interchanged (see text).

TABLE V. Comparison of the experimental lifetimes with our IBFFM calculation.

Level	Half-life Expt.[a]	IBFFM
$2^-(1)$	0.25(4) ns	0.13 ns
$1^-(1)$	0.52(14) ns	0.12 ns
$2^-(2)$	$\leq$0.01 ns	0.009 ns
$1^-(2)$	$\leq$7.7 ps	0.3 ps

[a]Experimental values taken from Ref. 27.

agreement with the experimental properties of ^{140}La, are boson-fermion dynamical interaction strengths $\Gamma_0(p)=\Gamma_0(n)=0.46$ MeV, spin-spin interaction strength $V_{\sigma\sigma}=0.13$ MeV, spin-spin-delta interaction strength $V_{\sigma\sigma\delta}=-0.02$ MeV, tensor interaction strength $V_T=-0.02$ MeV, and the hexadecapole-hexadecapole interaction strength $V_{44}=-0.18$ MeV. The energy pattern of the 14 lowest-energy levels in ^{140}La imposes very stringent conditions on the IBFFM parametrization. In searching for the correct parametrization, our guideline was the multiplet classification from Fig. 6, which arises in IBFFM as the leading-order perturbation effect due to the $\Gamma_0(p)$, $\Gamma_0(n)$, and $V_{\sigma\sigma}$ terms (*nota bene*: the relation of the parabolic rule to boson-fermion symmetry has been recently discussed in Ref. 22). The additional V_T term shifts the $0^-(1)$ state to a higher energy, while the V_{44} term keeps the $3^-(1)$ state at a low energy.

The results of our calculation for the low-energy negative-parity spectrum are presented in Fig. 7 and compared to the experimental levels and to the previously calculated spectra. All the IBFFM levels up to 0.6 MeV are assigned to experimentally known levels. These assignments were made taking into account the electromagnetic properties, transfer data, and the present results. Here we focus our consideration on the lowest two multipets that we observe in ^{140}La and elsewhere[39] we discuss the higher-energy levels.

In Tables III–V we compare the calculated electromagnetic properties of ^{140}La in IBFFM with the experimentally known level spectra and properties taken from the recent compilation of Peker[27] and our present results. The effective charges and gyromagnetic ratios used in the calculation have the standard values: $e^p=1.5$, $e^n=0.5$, $e^{\rm vib}=2.2$, $g_l(p)=1$, $g_l(n)=0$, $g_s(p)=0.6g_s(p,\text{free})$, $g_s(n)=0.6g_s(n,\text{free})$, and $g_R=Z/A=0.41$ (for a more complete definition of these parameters see Ref. 24).

V. DISCUSSION

The IBFFM wave functions of the low-lying states in Fig. 7 are dominated by two-quasiparticle components $|(pg_{7/2}nf_{7/2})J\rangle$ and/or $|(pd_{5/2}nf_{7/2})J\rangle$. For each state we present in Table VI the amplitudes associated with these two two-quasiparticle components. These amplitudes will be referred to as a_{gf} and a_{df}, respectively. On the basis of the largest component in each wave function, the IBFFM levels from Fig. 7 can clearly be classified into two multiplets, as shown in Fig. 8. In this figure the points (full circles) which present the IBFFM states are for each multiplet connected by a full line, and the points (triangles) which present the experimental levels by a dashed line.

In the wave functions of the $0^-(1)$ and $7^-(1)$ states, the $(pg_{7/2}nf_{7/2})$ component is the only component with $n_d=0$, but it amounts to nearly 90% of the total wave function. The wave functions of the levels $1^-(2)$, $2^-(1)$, and $1^-(1)$, $2^-(2)$ which are associated with the $(pg_{7/2}nf_{7/2})$ and $(pd_{5/2}nf_{7/2})$ multiplets, respectively, exhibit sizable mixing of these two two-quasiparticle components.

Due to the mixing of the two-quasiparticle components in the wave functions of the $1^-(1)$ and $1^-(2)$ states, the

TABLE VI. Absolute amplitudes of proton-neutron components $|(pg_{7/2}nf_{7/2})J\rangle$ and $|(pd_{5/2}nf_{7/2})J\rangle$ in the wave functions of the ^{140}La states.

	IBFFM		OOQM[a] $\lvert a(pn)\rvert$		TCF[b]	
Level	(gf)	(df)	(gf)	(df)	(gf)	Comment
$0^-(1)$	0.96		0.97		1.00	
$1^-(1)$	0.39	0.80	0.16	0.97	0.81	
$1^-(2)$	0.87	0.34	0.97	0.17	0.54	
$2^-(1)$	0.76	0.48	0.26	0.90	0.69	
$2^-(2)$	0.48	0.70	0.95	0.27	0.72	
$3^-(1)$	0.91	0.04	0.98	0.02	0.90	
$3^-(2)$	0.04	0.89	0.02	0.99	0.43	
$4^-(1)$	0.87	0.12	0.99	0.03	0.99	
$4^-(2)$	0.10	0.83	0.04	0.92	0.14	
$5^-(1)$	0.88	0.05	0.99	0.00	0.87	
$5^-(2)$	0.05	0.93	0.01	0.99	0.14	
$6^-(1)$	0.88	0.20	1.00	0.08	0.98	See note c.
$6^-(2)$	0.21	0.86	0.08	1.00	0.20	See note c.
$7^-(1)$	0.94		1.00		1.00	

[a]See Ref. 10.
[b]See Ref. 12.
[c]The sequence of the calculated 6^- states has been interchanged (see text).

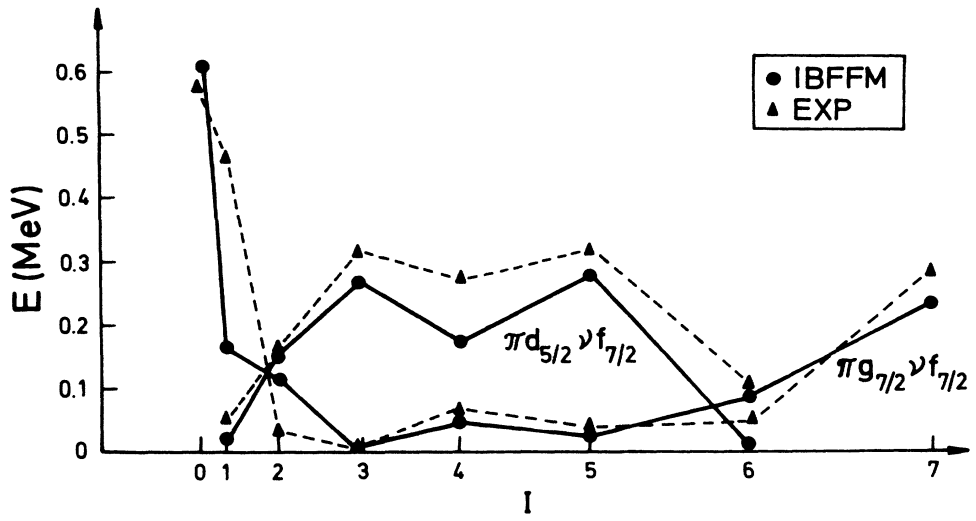

FIG. 8. Classification of the IBFFM levels into multiplets on the basis of largest components in the wave functions. The experimental levels of ^{140}La are compared with the theoretical spectra on the basis of level energies, electromagnetic deexcitation, and transfer properties. IBFFM and experimental levels are presented by solid circles and triangles, respectively.

$B(M1)$ values for both the $0^-(1)$ to $1^-(1)$ and $0^-(1)$ to $1^-(2)$ transitions are large, but the transition probability for the latter is sizably reduced with respect to the former due to the smaller transition energy. The remaining two transitions, depopulating the $0^-(1)$ to the $2^-(1)$ and $2^-(2)$ levels are even weaker because of the fifth power energy factor. Thus depopulation of the $0^-(1)$ state is dominated by the $0^-(1)$ to $1^-(1)$ transition.

The mixing between the two multiplets is, in particular, reflected in the decay pattern of the $1^-(2)$ state. Due to sizable mixing between the $pg_{7/2}nf_{7/2}$ and $pd_{5/2}nf_{7/2}$ components, the $B(M1)$ values for the transitions to the $2^-(1)$, $1^-(1)$, and $2^-(2)$ states are large (0.51, 0.47, and $2.12\mu_N^2$, respectively), and accordingly, the corresponding transition probabilities are large.

The ordering of the experimental levels agrees with the ordering of the calculated IBFFM levels for the states of all spins shown in Fig. 7, except for $J=6$. Namely, the lowest experimental 6^- level is strongly populated in the experimental (d,p) reaction, revealing that this state has a large amplitude of the $|(pg_{7/2}nf_{7/2})6\rangle$ component. On the other hand, the calculated second 6^- state has the largest $|(pg_{7/2}nf_{7/2})6\rangle$ component, and thus presents the counterpart of the lowest experimental 6^- level. Therefore, the first and second calculated 6^- states are assigned to the experimental $6^-(2)$ and $6^-(1)$ levels, respectively, as displayed in Fig. 7. Such an assignment, systematically employed in Tables III and IV, is in accordance with the observed branching ratios.

In Table VI the a_{gf} and a_{df} amplitudes are compared with the results of the OOQM calculation from Ref. 10 and the results of fitting the two-component ansatz to the experimental (d,p) amplitudes.[12] With respect to the ground state, it is interesting to note that the study of beta-gamma directional correlations[26] in the decay of ^{140}La indicates a value of $a_{df} \sim 0.04$, in agreement with the present calculation. As was pointed out in Ref. 10, the OOQM calculation underestimates the configuration mixing between the $pg_{7/2}$ and $pd_{5/2}$ configurations for spins 1, 2, and 3. Another problem of the OOQM calculation was posed by the 1^- states. Namely, the experimental data seem to indicate that the $1^-(1)$ state has $g_{7/2}$ as its largest proton component, while the OOQM calculation, in accordance with the Brennan-Bernstein rule, computed the largest proton component to be $d_{5/2}$. As seen from Table VI, the present IBFFM calculation improves the structure of the wave functions in both cases, but still the mixing appears too small. This is also seen in a comparison of the calculated and experimental branching ratios, which would improve by increasing the mixing in the wave functions. However, we have not succeeded in increasing the mixing further without distorting the energy pattern. It might be possible that additional interaction terms are needed in this respect.

VI. CONCLUSIONS

We have measured the deexcitation properties of levels in ^{140}La populated by the beta decay of ^{140}Ba using Compton-suppression techniques on sources whose daughter ^{140}La was continuously eluted by ion-exchange chromatography. The low-energy transitions between the low-energy levels have been studied by a measurement of the gamma rays ($E_x < 70$ keV) emitted after thermal neutron capture in ^{139}La. We have performed new theoretical investigations within the framework of the IBFFM and compared them to previous calculations. We find that the IBFFM calculation provides the best available description of the low-energy levels in ^{140}La. The higher-energy levels and the results of a comprehensive (*n*, gamma) and (n,e^-) study of high-energy gamma rays following thermal neutron capture in ^{139}La will be discussed elsewhere.[39]

ACKNOWLEDGMENTS

The authors wish to thank Professor O. W. B. Schult for his continuing support of our joint projects. This work was performed, in part, under the auspices of the U.S. Department of Energy by the Lawrence Livermore National Laboratory under Contract No. W-7405-Eng-48 and was supported in part by an Alexander von Humboldt fellowship. One of us (M.B.) wishes to acknowledge the financial support of the Internationales Büro of Kernforschungsanlage Julich.

---

*Permanent address: Division of High Energy and Nuclear Physics ER-23 GTN, Washington, D.C. 20545.

†On leave from Prirodoslovno-matematički fakultet, University of Zagreb, 41000 Zagreb, Yugoslavia.

[1]M. H. Brennan and A. M. Bernstein, Phys. Rev. **120**, 927 (1960).

[2]W. B. Walters, C. Chung, D. S. Brenner, A. Aprahamian, R. L. Gill, R. E. Chrien, M. Shmid, A. Wolf, and L.-J. Yuan, Phys. Lett. **125B**, 351 (1983).

[3]C. Chung, W. B. Walters, D. S. Brenner, A. Aprahamian, R. L. Gill, M. Shmid, R. E. Chrien, L.-J. Yuan, A. Wolf, and Z. Berant, Phys. Rev. C **28**, 2099 (1983).

[4]V. Paar, Nucl. Phys. **A331**, 16 (1979).

[5]B. H. Wildenthal, E. Newman, and R. L. Auble, Phys. Rev. C **3**, 199 (1971).

[6]B. S. Reehal and R. A. Sorensen, Phys. Rev. C **2**, 819 (1970).

[7]M. K. Pal and M. Mitra, Nucl. Phys. **42**, 221 (1963).

[8]L. Silverberg, Nucl. Phys. **60**, 483 (1964).

[9]L. S. Kisslinger and R. A. Sorensen, Rev. Mod. Phys. **35**, 853 (1963).

[10]G. L. Struble, Phys. Rev. **153**, 1347 (1967).

[11]H. C. Chiang, M. C. Wang, and S. T. Hseih, Nuovo Cimento Lett. **34**, 370 (1982).

[12]E. T. Jurney, R. K. Sheline, E. B. Shera, H. R. Koch, B. P. K. Maier, U. Gruber, H. Baader, D. Breitig, O. W. B. Schult, Y. Kern, and G. L. Struble, Phys. Rev. C **2**, 2323 (1970).

[13]A. Arima and F. Iachello, Phys. Rev. Lett. **35**, 157 (1975).

[14]F. Iachello and O. Scholten, Phys. Rev. Lett. **43**, 679 (1979).

[15]S. Brant, V. Paar, and D. Vretenar, Z. Phys. A **319**, 355 (1984).

[16]V. Paar, in *Capture Gamma-Ray Spectroscopy and Related Topics,* edited by S. Raman, (AIP, New York, 1985); V. Paar, S. Brant, D. Vretenar, D. K. Sunko, A. B. Balantekin, and T. Hübsch, in *Symmetries and Semiclassical Features of Nuclear Dynamics,* Vol. 279 of *Lecture Notes in Physics,* edited by A. A. Raduta (Springer-Verlag, Berlin, 1987).

[17]T. Hübsch and V. Paar, Z. Phys. A **319**, 111 (1984).

[18]T. Hübsch, V. Paar, and D. Vretenar, Phys. Lett. **151B**, 320 (1985).

[19]V. Lopac, S. Brant, V. Paar, O. W. B. Schult, H. Seyfarth, and A. B. Balantekin, Z. Phys. A **323**, 491 (1986).

[20]S. Brant, V. Paar, D. Vretenar, G. Alaga, H. Seyfarth, O. W. B. Schult, and M. Bogdanović, Phys. Lett. B **195**, 111 (1987).

[21]P. Van Isacker, J. Jolie, K. Heyde, and A. Frank, Phys. Lett. **54**, 653 (1985).

[22]A. B. Balantekin and V. Paar, Phys. Lett. **169B**, 9 (1986).

[23]D. Vretenar, S. Brant, and V. Paar, *The Computer Code* IBFFM, IKP Report No. 596679, IKP KFA-Julich (1985).

[24]V. Paar, S. Brant, L. F. Canto, G. Leander, and M. Vouk, Nucl. Phys. **A378**, 41 (1982).

[25]J. Van Maldeghem, J. Sau, and K. Heyde, Phys. Lett. **116B**, 387 (1982).

[26]K. W. Kemper, R. D. Murphy, and R. G. Wilkinson, Nucl. Phys. **A124**, 298 (1969).

[27]L. K. Peker, Nucl. Data Sheets **51**, 395 (1987).

[28]T. W. Burrows, Nucl. Data Sheets **52**, 273 (1987).

[29]L. K. Peker, Nucl. Data Sheets **36**, 289 (1982).

[30]L. K. Peker, Nucl. Data Sheets **43**, 570 (1984).

[31]J. K. Tuli, Nucl. Data Sheets **27**, 97 (1979).

[32]L. K. Peker, Nucl. Data Sheets **41**, 195 (1984).

[33]A. Ercan, KFA-Julich Report No. Jul-Spez-189, ISSN 0343-7639, Julich, F.R. Germany, 1983.

[34]K. Debertin, U. Schotzig, and K. F. Walz, Nucl. Sci. Eng. **64**, 784 (1977).

[35]J. T. Harvey, J. L. Maeson, J. C. Hogan, and H. L. Wright, Nucl. Sci. Eng. **58**, 431 (1975).

[36]C.-C. Lin, J. Inorg. Nucl. Chem. **38**, 1409 (1976).

[37]R. J. Gehrke, R. G. Helmer, and R. C. Greenwood, Nucl. Instrum. Methods **147**, 405 (1977).

[38]I. Adam, N. M. Anton'eva, V. B. Brudanin, M. Budzynski, Ts. Vylov, N. A. Dzhashi, A. Zhumamuratov, A. I. Ivonov, V. G. Kalinnikov, A. Kugler, V. V. Kuznetsov, Li Zon Sik, T. M. Muminov, A. F. Novgorodov, Yu. N. Podkopaev, Z. D. Shavgulidze, and V. L. Chikhladze, Izv. Akad. Nauk SSSR Ser. Fiz. **46**, 2 (1982).

[39]M. Bogdanović, J. Simić, M. P. Stojanović, R. Vukanović, M. Župančić, H. G. Börner, G. Colvin, F. Hoyler, K. Schreckenbach, H. Seyfarth, S. Brant, V. Paar, and R. A. Meyer (unpublished).

[40]M. Bogdanović, J. Simić, M. P. Stojanović, R. Vukanović, M. Župančić, H. G. Börner, G. Colvin, F. Hoyler, K. Schreckenbach, H. Seyfarth, S. Brant, and V. Paar, in *Capture Gamma-Ray Spectroscopy 1987,* edited by K. Abrahams and P. van Assche, Inst. Phys. Conf. Ser. No. 88 (IOP, Bristol, England, 1988), p. 553.

[41]H. G. Hicks, Lawrence Livermore National Laboratory, Report No. UCID-52968, Nuclear Chemistry Division Internal Report, 1979 (unpublished).

[42]D. C. Camp, in *Proceedings of the International Conference on Radioactivity in Nuclear Spectroscopy,* edited by J. H. Hamilton and J. C. Manthuruthil (Gordon and Breach, New York, 1971), p. 381.

[43]R. A. Meyer, Multigamma-Ray Standards, LLNL Manual, M-100 (1979).

[44]R. A. Meyer and T. N. Massey, Int. J. Appl. Radiat. Isot. **34**, 1073 (1983).

[45]R. Gunnink and J. B. Niday, UCRL-51061, 1972.

[46]W. Delang, P. Göttel, and H. Seyfarth, Nucl. Instrum. Methods **99**, 13 (1972).

[47]S. F. Mughabghab, M. Divadeenam, and N. E. Holden, *Neutron Cross Sections* (Academic, New York, 1981), Vol. I.

[48]H. Seyfarth, S. Brant, P. Göttel, V. Paar, D. Vorkapić, and D. Vretenar, Z. Phys. A **330**, 141 (1988).

[49]E. G. Kessler, Jr., R. D. Deslattes, A. Henins, and W. C. Sauder, Phys. Rev. Lett. **40**, 171 (1978).

[50]J. Kern and G. Mauron, Helv. Phys. Acta **43**, 272 (1970).

[51]R. Weishaupt and D. Rabenstein, Z. Phys. **251**, 105 (1972).
[52]H. H. Schmidt, P. Hungerford, H. Daniel, T. von Egidy, S. A. Kerr, R. Bissot, G. Barreau, H. G. Börner, C. Hofmeyr, and K. P. Lieb, Phys. Rev. C **25**, 2888 (1982).
[53]C. M. Baglin, Nucl. Data Sheets **30**, 1 (1980).
[54]*Table of Isotopes*, 7th ed., edited by C. M. Lederer and V. S. Shirley (Wiley, New York, 1978).
[55]S. I. Salem, S. L. Panossian, and R. A. Krause, At. Data Nucl. Data Tables **14**, 91 (1974).
[56]J. H. Scofield, At. Data Nucl. Data Tables **14**, 121 (1974).
[57]F. P. Larkins, At. Data Nucl. Data Tables **20**, 311 (1977).
[58]M. P. Fioratti and S. R. Piermattei, Nucl. Instrum. Methods **96**, 605 (1971).

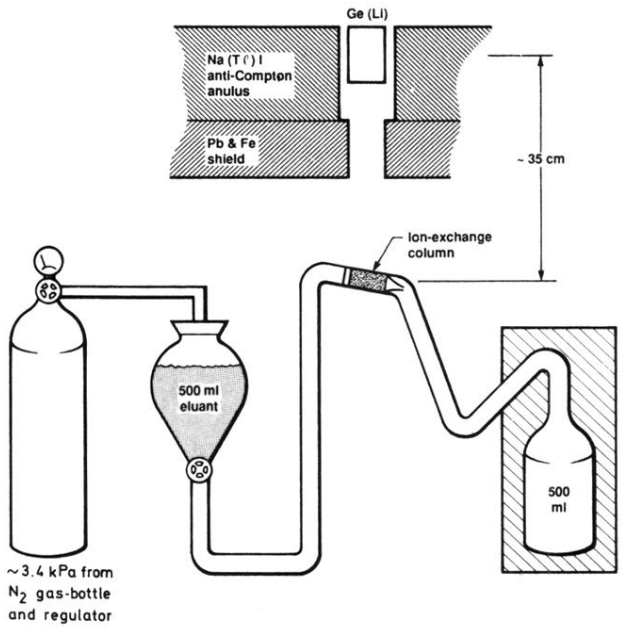

FIG. 2. Diagrammatic sketch of the experimental setup for measuring the Compton-suppression spectra of a ^{140}Ba-^{140}La source in which the daughter ^{140}La activity was continuously eluted from the ^{140}Ba parent activity. The ^{140}Ba activity, contained on the ion-exchange resin, was eluted with a solution of alcoholic alpha-But under a pressure of $\sim\frac{1}{2}$ psi. The column was aligned with the central axis of the Compton-suppression spectrometer's aperture (see text).